NeuroImage 44 (2009) 715–723

Contents lists available at ScienceDirect

NeuroImage

journal homepage: www.elsevier.com/locate/ynimg

Age-related changes in modular organization of human brain functional networks

David Meunier [a,b], Sophie Achard [a,b,c], Alexa Morcom [d], Ed Bullmore [a,b,*]

[a] Brain Mapping Unit, University of Cambridge, Cambridge, UK
[b] Behavioural and Clinical Neurosciences Institute, University of Cambridge, Cambridge, UK
[c] Grenoble Image Parole Signal Automatique, Centre National de la Recherche Scientifique, Grenoble, France
[d] Centre for Cognitive and Neural Systems, University of Edinburgh, Edinburgh, UK

ARTICLE INFO

Article history:
Received 21 May 2008
Revised 4 September 2008
Accepted 30 September 2008
Available online 5 November 2008

Keywords:
Aging
Complex networks
Functional MRI
Modularity

ABSTRACT

Graph theory allows us to quantify any complex system, e.g., in social sciences, biology or technology, that can be abstractly described as a set of nodes and links. Here we derived human brain functional networks from fMRI measurements of endogenous, low frequency, correlated oscillations in 90 cortical and subcortical regions for two groups of healthy (young and older) participants. We investigated the modular structure of these networks and tested the hypothesis that normal brain aging might be associated with changes in modularity of sparse networks. Newman's modularity metric was maximised and topological roles were assigned to brain regions depending on their specific contributions to intra- and inter-modular connectivity. Both young and older brain networks demonstrated significantly non-random modularity. The young brain network was decomposed into 3 major modules: central and posterior modules, which comprised mainly nodes with few inter-modular connections, and a dorsal fronto-cingulo-parietal module, which comprised mainly nodes with extensive inter-modular connections. The mean network in the older group also included posterior, superior central and dorsal fronto-striato-thalamic modules but the number of intermodular connections to frontal modular regions was significantly reduced, whereas the number of connector nodes in posterior and central modules was increased.

Introduction

Modularity is a word with many meanings in neuroscience (Fodor, 1983; Zeki and Bartels, 1998; Redies and Puelles, 2001; Callebaut and Rasskin-Gutman, 2005). Here we are concerned with the topological organization of whole human brain functional networks and the partitioning of these networks into a set of modules, each module being defined by dense internal or intra-modular connectivity and relatively sparse external or inter-modular connectivity (Newman and Girvan, 2004); see Fig. 1. This pattern of complex network organization, also sometimes described as a community structure, is widespread in biochemical, social and infrastructural networks (Guimerà et al., 2005). A key advantage of modular organization, which may explain its ubiquity in diverse systems, is that it favours evolutionary and developmental optimization of multiple or changing selection criteria (Redies and Puelles, 2001; Slotine and Lohmiller, 2001; Kashtan and Alon, 2005; Pan and Sinha, 2007): a modular network can evolve or grow one module at a time, without risking loss of function in other modules.

Mathematical tools have recently been developed to quantify the modularity of any network that can be abstractly described as a set of nodes and links (Newman and Girvan, 2004; Newman, 2004a; Danon et al., 2005; Newman, 2006). Once the modules have been identified, this information can be further used to refine the definition of the topological role of any particular node. For example, the global air transportation network has a modular organization (Guimerà and Amaral, 2005b), broadly conforming to geopolitical constraints, which informed the assignment of distinct roles to the component nodes (cities) based on the ratio of intra- and inter-modular links (flights) connecting each node to the rest of the network. Thus a highly-connected city, like London, with many long-haul flights to other modules (different continents), was designated a *connector* hub; whereas a regionally important city, like Barcelona, with relatively few long-haul flights outside Europe and North Africa, was designated a *provincial* hub.

Here we extend the analysis of modularity and topological roles in functional brain networks, using tools drawn from the literature on physics of complex networks (Newman and Girvan, 2004; Guimerà and Amaral, 2005b) that have not been previously applied to analysis of human functional neuroimaging data. However, we note that there have been several prior studies using conceptually related multivariate or graph theoretical methods to explore the clustered or modular organization of mammalian cortex. Young (1992) applied non-metric multidimensional scaling (MDS) to anatomical connectivity matrices to demonstrate dorsal and ventral "streams" of inter-regional connectivity, and a predominance of local neighbourhood

* Corresponding author. Brain Mapping Unit, University of Cambridge, Department of Psychiatry, Addenbrooke's Hospital, Cambridge CB2 2QQ, UK. Fax: +44 1223 336581.
E-mail address: etb23@cam.ac.uk (E. Bullmore).

1053-8119/$ – see front matter.
doi:10.1016/j.neuroimage.2008.09.062

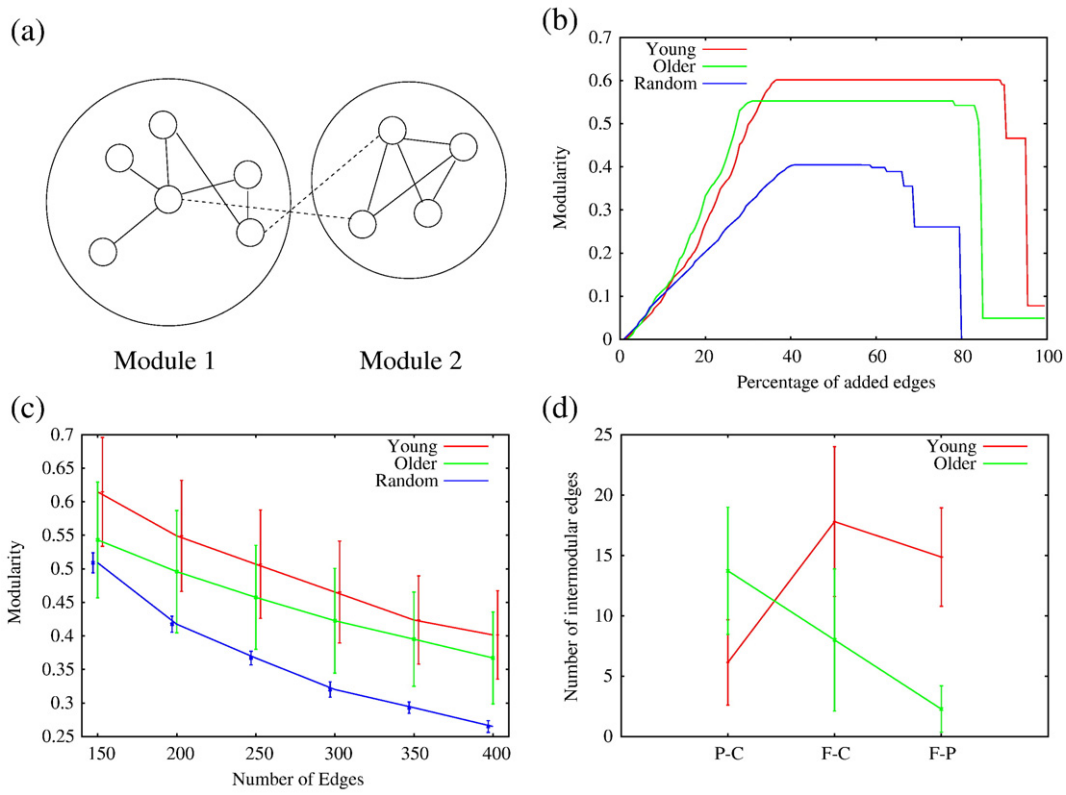

Fig. 1. (a) Schematic illustration of modularity. By definition, modules have relatively sparse external or intermodular connectivity. (b) Modularity optimization process for group mean young (red), group mean older (green) and example random (blue) networks with 200 links. (c) The maximum modularity achieved for young (red), older (green) and random (blue) networks, with number of links between 150 and 400. The maximum modularity was estimated for each individual network and the 95% confidence intervals therefore represent the variability between subjects with respect to the mean in each age group. (d) Number of links between the three main modules obtained for individually estimated young and older networks with 200 links: F = fronto-cingulo-parietal (young) or dorsal fronto-striato-thalamic (older); C = central (young) or superior central (older); P = posterior. Error bars are 95% confidence intervals for the mean number of links in each age group.

connections, in primate visual cortex. Scannell et al. (1995, 1999) and Hilgetag et al. (2000) applied non-metric MDS, non-parametric cluster analysis (NPCA), and a novel evolutionary algorithm called optimal set analysis (OSA), to show that the anatomical connectivity of the cat and macaque cortices demonstrated relatively dense connections within groups of functionally related regions and much sparser connections between different groups of regions. Stephan et al. (2000) investigated neuronographic data, which mapped the propagation of epileptiform activity following local disinhibition of areas of the macaque cortex by topical application of strychnine, and showed that functionally connected regions of cortex tended to co-segregate in one of three major sub-systems (visual, somatomotor, or orbito-temporo-insular). Various forms of hierarchical cluster analysis were subsequently applied to human functional MRI data acquired in a no-task or resting state (Cordes et al., 2002; Salvador et al., 2005). For example, Salvador et al. (2005) showed that 90 cortical and subcortical regions defined by an anatomically parcellated template image were aggregated by cluster analysis into 6 major systems of anatomically and functionally related regions. More recently, using graph theoretical tools, the community structure of human brain networks has been investigated using structural MRI to infer anatomical connectivity between major cortical and subcortical regions (Chen et al., 2008). This study confirmed that the human brain anatomical network, derived from analysis of MRI data on a large group of healthy volunteers, had a modular organization which broadly conformed to known functional specialisations and the hierarchical cluster solution reported by Salvador et al. (2005); for example, many occipital regions specialised for visual processing were identified as members of the same anatomical module. There have also been a few recent graph theoretical studies of modularity of functional networks inferred from fMRI measurements on rodents (Schwarz et al., 2008) and healthy human adults (Ferrarini et al., in press).

In this context, the distinctive contributions of this paper are to apply a graph-theoretical measure of modularity (Newman and Girvan, 2004), and related concepts of the topological roles of individual nodes (Guimerà and Amaral, 2005b), to the analysis of human functional MRI data, with two main objectives: i) to further investigate the modular organization and topological roles of each regional node comprising large-scale human brain functional networks; and ii) to test the hypothesis that normal aging is associated with changes in the community structure of whole human brain functional networks.

Materials and methods

Sample

Thirty healthy human volunteers were recruited in two age groups: 17 younger participants aged 18–33 years, mean age=24.3 years, nine male; and 13 older participants aged 62–76 years, mean age=67.3 years, six male. Recruitment was via local advertising followed by telephone screening using a standard questionnaire. Exclusion criteria included a history of neurological or psychiatric disorder, current treatment with vasoactive or psychotropic medication, or any contraindication to MRI. Prior to functional MRI, each participant had an electrocardiogram and a structural MRI examination reviewed as normal by a physician.

The two age groups were matched on education and crystallised IQ, as estimated by the National Adult Reading Test (NART; (Nelson, 1982)). Older volunteers also completed the Mini Mental State

Examination (Folstein et al., 1975) and scored ≥28 (maximum score = 30) to be eligible for participation.

All participants gave informed consent in writing. The study was approved by the Addenbrooke's NHS Trust Local Research Ethics Committee, Cambridge, UK.

A different analysis of data acquired on this sample has been previously reported (Achard and Bullmore, 2007).

Functional MRI data acquisition and pre-processing

Each participant was scanned lying quietly at rest with eyes closed for 9 min, 37.5 s. Gradient echo, ecoplanar imaging (EPI) data depicting BOLD contrast were acquired using a Medspec S300 scanner (Bruker Medical, http://bruker-medical.de) operating at 3.0 T in the Wolfson Brain Imaging Centre, Cambridge, UK. We acquired 525 volumes with the following parameters: number of slices, 21 (interleaved); slice thickness, 4 mm; interslice gap, 1 mm; matrix size, 64×64; flip angle, 90; repetition time (TR), 1100 ms; echo time, 27.5 ms; in-plane resolution, 3.125 mm. The first seven volumes were discarded to allow for T1 saturation effects, leaving 518 volumes available for analysis of endogenous, low frequency brain dynamics recorded in a no-task or resting state condition.

Each dataset was corrected initially for geometric displacements due to head movement and co-registered with the Montreal Neurological Institute EPI template image, using an affine transform implemented in SPM2 software (http://www.fil.ion.ucl.ac.uk). Four datasets (two young, two old) that had been affected by head movement in excess of 3 mm translation or 0.3 rotation in any dimension were discarded. The remaining data were not spatially smoothed before regional parcellation using a previously validated, anatomically labelled template image (Tzourio-Mazoyer et al., 2002). This parcellation divides each cerebral hemisphere into 45 anatomical regions. Regional mean time series were estimated for each individual by averaging the fMRI time series over all voxels in each of 90 regions. Each regional mean time series was further corrected for the effects of head movement by regression on the time series of translations and rotations of the head estimated in the course of initial movement correction by image registration. The residuals of these regressions constituted the set of regional mean time series used for wavelet correlation analysis.

Wavelet correlation analysis and network construction

Frequency-dependent functional connectivity between each pair of regional time series was estimated using wavelet correlations, as previously described (Whitcher et al., 2000; Achard et al., 2006; Bassett et al., 2006; Achard et al., 2008). In brief, we used the maximal overlap discrete wavelet transform (MODWT) to decompose each regional mean time series into wavelet coefficients at four scales or frequency intervals. Then we estimated the pairwise inter-regional correlations between wavelet coefficients at each scale. This resulted in a set of four {90×90} scale-specific wavelet correlation matrices for each of the $m = 1,2,3,\ldots, M$ subjects in the sample. To summarize functional connectivity maps on average over all subjects within each group, we also computed the group mean wavelet correlation matrix at each scale for the young and older participants. Because of prior data indicating that correlated endogenous dynamics in resting state fMRI data are particularly salient at frequencies below 0.1 Hz (Lowe et al., 1998; Cordes et al., 2000), we restricted our attention to the scale 3 wavelet correlation matrices representing functional connectivity in the frequency interval 0.06–0.11 Hz.

To analyse graphical properties of brain functional networks, each wavelet correlation matrix (whether estimated for a single subject or averaged over a group of subjects) must be thresholded to create an adjacency matrix A, the a_{ij}^{th} element of which is either 1, if the absolute value of the wavelet correlation between nodes i and j exceeds a threshold value τ; or 0, if it does not. For this purpose, we defined a range of thresholds to satisfy two opposing constraints. First, we confirmed by preliminary analysis the theoretically expected result that low thresholds, with high connection densities, would generate graphs with low modularity equivalent to a random graph. This typically occurred when the total number of edges in the graph exceeded 400, which was therefore used to define the lower limit of the threshold range. However, we also observed that very high thresholds, with low connection densities, could generate disconnected graphs in which some regions were not linked to any other brain region. Theoretically (Bollobas, 1985), fragmentation of a random network is likely to occur when the connection density of the graph, i.e. the number of links divided by the maximum possible number of links, is greater than $1/N$, where N is the number of nodes in the network. In our case, $N = 90$, thus the number of links must be greater than $1/N{*}N(N-1)/2 = (N-1)/2 \sim 50$. To ensure that all networks were fully connected, we conservatively defined the upper limit of the threshold range as equivalent to a minimum of 100 edges in the thresholded graph. In short, we investigated network modularity over a range of thresholds designed to focus on fully-connected but non-random aspects of brain network organization.

Topological properties of brain networks such as modularity can be quantitatively compared to the equivalent properties of comparable random networks. Such networks were generated by starting with a set of unconnected nodes the same size as the brain network ($N = 90$) and randomly adding edges or links between pairs of nodes under a uniform probability distribution (the probability of adding an edge is equal for all possible pairs) until the number of edges in the random network was within the range $L = 100$–400 links or edges.

Modularity and role assignment

A module can be generally defined as a subset of nodes in the graph which are more densely connected to the other nodes in the same module than to nodes outside the module (Radicchi et al., 2004); see Fig. 1(a). Several algorithms have been proposed to define the modular decomposition of an undirected graph (Newman and Girvan, 2004; Newman, 2004b; Clauset et al., 2004; Guimerá et al., 2004; Guimerà and Amaral, 2005a,b; Reichardt and Bornholdt, 2006). Here we have adopted Newman's metric as a measure of modularity (Newman and Girvan, 2004; Guimerá et al., 2004; Danon et al., 2005) and maximised this measure by a "greedy" search algorithm (Clauset et al., 2004).

First we define the degree of the ith node, k_i, as the number of links or edges connecting it to all other nodes in the network. Then, for a set of N_M modules in a graph defined by a particular threshold, the modularity measure is

$$M = \sum_{s=1}^{N_M} \left[\frac{l_s}{L} - \left(\frac{d_s}{2L} \right)^2 \right] \quad (1)$$

where N_M is the number of modules, L is the total number of links or edges in the network, ls is the total number of links between nodes in module s, and ds is the sum of the degrees of the nodes in module s.

The modularity of the network will be low before addition of any links, when each node is isolated (equivalent to very high thresholds); it will be zero when all possible connections between nodes have been made and all nodes are part of a single module (equivalent to very low thresholds); and for some intermediate number of links, the modularity will have a maximum value. It is generally accepted that maximal values of $M \geq 0.3$ are indicative of non-random community structure (Newman and Girvan, 2004). However, random networks can demonstrate considerable degrees of modularity especially when they are sparsely connected (Guimerá et al., 2004). In term of computational complexity, rigorous optimization of modularity is a so-called "NP-hard" problem (Brandes et al., 2006). Various methods have been proposed to find the optimally modular decomposition of a

complex network in a computationally feasible way. Some algorithms use the concept of link centrality to incrementally increase network modularity to a maximum (Newman and Girvan, 2004); alternatively it is possible to search directly for the global maximum modularity using standard numerical optimization algorithms such as the "greedy" algorithm (Newman, 2004a,b; Clauset et al., 2004) or simulated annealing (Guimerà et al., 2005; Massen and Doye, 2005).

The greedy algorithm involves rebuilding the network by serially adding links in order to maximise, at each step, the value of modularity. Its basic assumption is that finding the local maximum at each step is an heuristic to find the global maximum. This assumption is not entirely reliable, so other optimization algorithms, such as simulated annealing, are more likely to find the true global maximum but are correspondingly more costly in terms of computational time. The greedy algorithm was used here because it provides a reasonable trade-off between global optimality and expediency (Boccaletti et al., 2007). Fig. 1 in Supplementary material shows that results with Newman and Girvan method, and with simulated annealing algorithm are very close to those obtained with greedy algorithm. The results of applying this algorithm to analysis of the community structure in representative individual (young and older) brain functional networks, and a comparable random network, are shown in Fig. 1(b).

Once a maximally modular partition of the network has been identified, it is possible to assign topological roles to each node based on its density of intra- and inter-modular connections (Guimerà et al., 2005; Guimerà and Amaral, 2005a,b; Sales-Pardo et al., 2007). Intra-modular connectivity is measured by the normalized intra-modular degree:

$$z_i = \frac{\kappa_{n_i} - \overline{\kappa}_n}{\sigma_{\kappa_n}} \tag{2}$$

where κ_{n_i} is the intra-modular degree of the ith node, i.e., it is the number of links connecting the i^{th} node in the n^{th} module to other nodes in the same module; $\overline{\kappa}_n$ is the average intra-modular degree over all nodes in the n^{th} module; and σ_{κ_n} is the standard deviation of the intra-modular degrees in the n^{th} module. Thus $z_i$will be large for a node that has a large number of intra-modular connections relative to other nodes in the same module.

Inter-modular connectivity is measured by the participation coefficient:

$$P_i = 1 - \sum_{n=1}^{N_M} \left(\frac{\kappa_{n_i}}{k_i}\right)^2 \tag{3}$$

where κ_{n_i} is the intra-modular degree as previously defined, and k_i is the total degree of the i^{th} node. Thus P_i will be close to one if it is extensively linked to all other modules in the community and zero if it is linked exclusively to other nodes in its own module.

The two-dimensional space defined by these parameters, the *z-P* plane, can be arbitrarily partitioned to assign categorical roles to the nodes of the network. Thus for large networks, 7 different categorical roles were assigned (Guimerà et al., 2005); but for the smaller brain networks considered here we partitioned the plane into four domains and assigned roles according to the following criteria:

- If $P_i > 0.05$, node *i* was defined as a *connector* node; otherwise, it was defined as a *provincial* node. Note that this criterion simply segregates (provincial) nodes with no inter-modular connections from (connector) nodes with one or more intermodular connections.
- If $z_i > 1.0$, node *i* was defined as a *hub*; otherwise, it is defined as a *non-hub*. Note that this criterion segregates nodes with somewhat greater than average intramodular degree from nodes with intramodular degree close to or less than the modular average.

Thus the four possible roles were connector hub, connector non-hub, provincial hub and provincial non-hub. Likewise, the topological role of each module can be defined in terms of the proportion of connector nodes it contains and the number of links that connect it to each other module in the network.

Statistical testing of differences between brain network parameters and comparable random network parameters, and of differences between young and older brain network parameters, was conducted using standard parametric models (analysis of variance, ANOVA) after establishing by Kolmgorov–Smirnov tests that all the test statistics considered had an approximately Normal distribution.

Results

Human brain functional networks are modular

Brain functional networks were consistently modular in both age groups and over a range of different thresholds or connection densities; see Fig. 1(c). For both age groups, as well as for comparable random networks, maximum modularity declined monotonically as a function of increasing connection density, i.e., maximum modularity was greatest for the sparsest networks considered. However, over the entire range of connection densities, the modularity of both the young and older brain networks was significantly greater than random: for young brain networks *versus* random networks, ANOVA, $F(1,28) = 48.41$, $p < 10^{-6}$; for older brain networks *versus* random networks, ANOVA, $F(1,24) = 19.732$, $p = 0.0002$. There was no significant difference in modularity of young and older brain networks, ANOVA, $F(1{:}24) = 2.54$, $p = 0.124$. There was also no significant interaction between age and connection density (ANOVA, $F(5{:}20) = 1.385$, $p = 0.272$), indicating that the modularity of young and older brain networks can be compared at any connection density.

More fine-grained analysis was subsequently focused on the community structure arising in young and older brain networks with 200 links, i.e. thresholded at a sparse connection density equivalent to about 5% of the total number of possible links (4005) in a network of 90 nodes; see Fig. 1(b). The maximum modularity of this network was $M(Y) = 0.61$ for the young group and $M(O) = 0.55$ for the older group; the maximum modularity of a comparable random graph was $M(R) = 0.4$; see Fig. 1(b). For both young and older brain networks, maximum modularity at this connection density was significantly greater than the modularity of the random graphs: for young brain networks *versus* random networks, ANOVA, $F(1,28) = 37.248$, $p = 1.39 \times 10^{-6}$; for older brain networks *versus* random networks, $F(1,24) = 10.981$, $p = 0.0029$.

Modules and node roles in young brain functional networks

The young brain functional network comprised 5 connected modules, which varied in size from 24 to 2 regional nodes; see Fig. 2(a).

The largest module (24 regions) included bilateral pre- and post-central gyri and supplementary motor area, as well as several regions of lateral temporal cortex and insula, and was therefore designated the "central" or C module. The second largest module (22 regions) included bilateral and medial dorsal prefrontal cortex; anterior, dorsal and posterior cingulate cortex; medial posterior parietal cortex; a few regions of temporal cortex; caudate nucleus and thalamus, and was designated the "fronto-cingulo-parietal" or F module. The third largest module (18 regions) included bilateral calcarine cortex and all other regions of occipital cortex and was designated the "posterior" or P module. Relatively minor modules included a ventral frontal module, comprising 6 regions of bilateral inferior frontal gyrus and orbito-frontal cortex, and a medial temporal module composed of left amygdala and left hippocampus. See Fig. 2 for representations of the community structure in anatomical (c and d) and topological spaces (e and f). The topological representation uses the Kamada–Kawai (Kamada and Kawai, 1989) algorithm, that minimizes the physical distances between nodes according to their topological distances. Basically, the free energy is based on the difference between physical

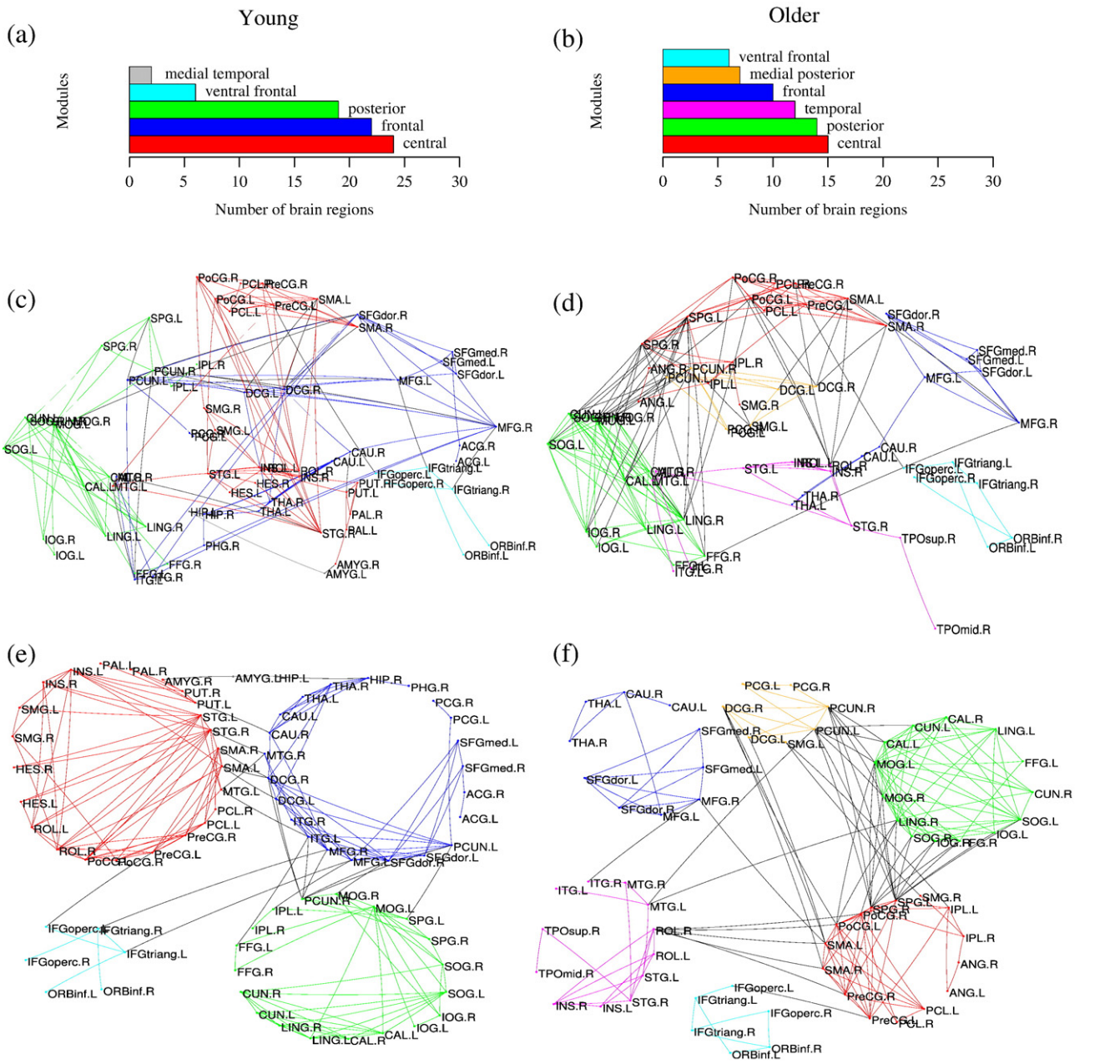

Fig. 2. Community structure for young and older brain functional networks. Upper: Histograms of the number of nodes in modules for average young (a) and older (b) networks comprising 200 links each. Middle: Anatomical representations for average young (c) and older (d) population networks. Lower: Topological representation (minimizing free energy) for average young (e) and older (f) brain networks.

distance between a pair of nodes in the representation of the graph and the shortest path between these pair of nodes. By minimising this free energy, the physical representation will take into account the topological distances existing between pairs of nodes.

Almost half (10/22) of the brain regions comprising the fronto-cingulo-parietal module had numerous connections to other modules, and were therefore categorised as connector nodes, i.e., the connector coefficient for the F module was 10/22=45%; see Figs. 3 (a) and (c). Five regions (left precuneus, right dorsal superior frontal gyrus, right dorsal cingulate gyrus, and bilateral middle frontal gyri) were categorised as connector hubs because they also had a high density of intramodular connections. Overall, 22% (5/22) of F module nodes were classified as hubs, and these were all connectors.

For regions comprising both the central and posterior modules, the profile of topological roles was markedly different. For the central module, most (17/24) regions did *not* have connections to regions in different modules, and were therefore categorised as provincial nodes, including 4 provincial hubs with high intramodular degree; only 7/24 regions were categorised as connector nodes, including 1 connector hub (right superior temporal gyrus), so the connector coefficient for the C module was 7/24=29%. Likewise, for the posterior module, most (11/15) regions were categorised as provincial nodes, including 2 provincial hubs (left middle and superior occipital gyrus); only 5/19 regions were categorised as connector nodes, with no connector hubs, so the connector coefficient for the P module was 26%, i.e., much smaller than for the F module.

In short, we found 3 major modules (see Table 1 in Supplementary material) in the young brain functional network which could be clearly distinguished by their profile of intermodular connectivity. The fronto-cingulo-parietal module was more highly connected externally – it was

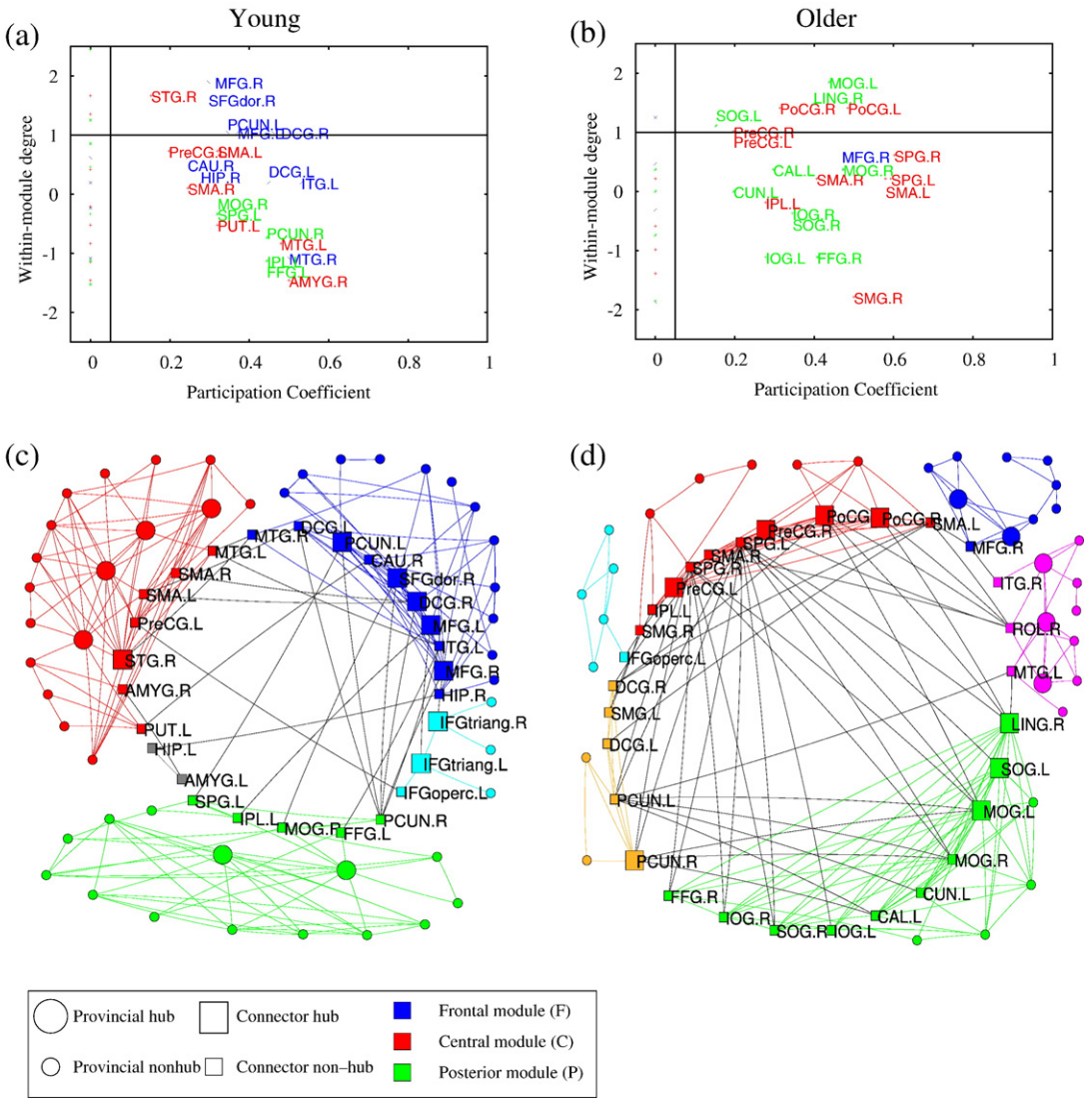

Fig. 3. Brain modules and regional node roles for young and older brain functional networks. Upper: Within-module degree as described by Eq. (2) (*y*-axis) *versus* participation coefficient as described by Eq. (3) (*x*-axis) for each of the regional nodes comprising the three main (F, C, P) modules in young (a) and older (b) brain networks. The solid vertical line divides the plane into connector nodes (right; anatomically labelled) and provincial nodes (left); the solid horizontal line divides the plane into hubs (above) and non-hubs (below). Lower: Topological representation of the average young (c) and older (d) brain networks with connector nodes located in a central ring to highlight intermodular connections.

a connector module – whereas the central and posterior modules were more highly connected internally — they were provincial modules.

Modules and node roles in older brain functional networks

By comparison to the community structure of the young brain network, there were clear differences in relative size and topological role profile of most of the modules in the mean brain network for the older group. The network for the older group comprised 6 connected modules, which varied in size from 15 to 6 regional nodes; see Fig. 2 (b). The largest module (15 nodes) comprised bilateral regions of precentral, premotor, somatosensory and parietal association cortex and was designated “superior central”. The second largest module (14 nodes) comprised almost exactly the same set of regions of occipital cortex as the young posterior module and was therefore also designated “posterior”. The third largest module (12 regions) comprised regions of lateral temporal cortex and insula and was designated “temporal”. The fourth largest module (10 nodes) comprised dorsal and medial prefrontal cortex, caudate and thalamus and was therefore designated “fronto-striato-thalamic”. The fifth largest module (7 nodes) comprised regions of medial posterior parietal cortex, dorsal and posterior cingulate cortex, and was therefore designated “medial posterior”. The smallest module (6 nodes) comprised the same set of ventral prefrontal and orbitofrontal cortex as in the young network and was therefore also designated “ventral frontal”.

In short, the regions comprising the large dorsal fronto-cingulo-parietal module of the young brain network had segregated into two smaller and more local modules in the older group's mean network — a dorsal prefronto-striato-thalamic module and a medial posterior module. Likewise the regions comprising the large central module of the young brain network had segregated into two smaller and more local modules in the older group's mean network — a lateral temporo-insular module and a superior central module. In contrast, the posterior and ventral frontal modules of the young brain network were conserved almost identically in the older group's mean network.

In addition to these differences in module size and composition, there were also changes in the topological roles of regions and modules (see Table 2 in Supplementary material). The fronto-striato-thalamic module included a smaller proportion of connector nodes (1/10; and no connector hubs) so its connector coefficient was only

10%, i.e., about 78% smaller than that of the fronto-cingulo-parietal module in young people; see Figs. 3(b) and (d). On the other hand, both posterior and superior central modules had greater intermodular connectivity than the comparable (posterior and central) modules in the young brain network. Thus the connector coefficient was 71% for the posterior module, and 66% for the superior central module, in the older group's mean network (see Tables 3 and 4 in Supplementary material).

By inspection of Fig. 3, it is clear that the young brain network was characterised by a lack of direct intermodular (P-C) connections between posterior and central modules, with relatively dense intermodular connections between the fronto-cingulo-parietal module and both posterior (F-P) and central (F-C) modules. Whereas, in the older group's mean network, there was relatively dense intermodular connectivity between posterior and superior central or medial posterior modules, and a relative paucity of intermodular connections to the dorsal fronto-striato-thalamic module. Noting that superior central and dorsal fronto-striato-thalamic modules in the older group's mean brain network represent subsets of the central and fronto-cingulo-parietal network in the young brain network, and that the posterior module was almost identical in the two groups, we calculated the number of links between these three modules in the network for each subject separately; see Fig. 1 (d). There was a significant interaction between age and intermodular connection profile (ANOVA, $F(1,24)=10.42$, $p=0.0006$). Post-hoc tests demonstrated significant between-group differences in the number of links or edges between all possible pairs of modules: links between posterior and central modules were increased in older people (ANOVA, $F(1,24)=5.94$, $p=0.022$) whereas links between frontal and posterior modules (ANOVA, $F(1,24)=23.82$, $p=5.62\times10^{-5}$) and between frontal and central modules (ANOVA, $F(1,24)=4.72$, $p=0.039$), were significantly reduced in older people.

Discussion

These results illustrate how graph theoretical techniques from the statistical physics literature can be used to characterise the modular organization of human brain functional networks. For both young and older brain networks, maximum modularity, as defined by the Newman and Girvan (2004) algorithm, was significantly greater than in comparable random graphs. Although technically novel, this observation is arguably not too surprising when we recall the long-standing arguments and evidence in favour of modular organization of brain function; and, more specifically, that (non-random Newman's) modularity of whole brain networks has been previously reported on the basis of human structural MRI (Chen et al., 2008) and rat functional MRI (Schwarz et al., 2008) studies, using similar mathematical tools from graph theory. Modular systems generally have the advantage of allowing evolutionary or developmental adaptation of one functional module, without risking loss of function in other modules, and have been shown to represent an efficient solution to multiple selection pressures on network evolution (Kashtan and Alon, 2005). It is also recognised that modular systems will often have small-world properties of high clustering and short path length at a global level of description, and there is increasing evidence for small-world organization of human brain networks; see Bassett and Bullmore (2006) for review. For all of these reasons, modularity of large-scale human fMRI networks was theoretically expected. However, we have taken the investigation of brain functional modularity further in two main ways.

First, we have considered the topological roles of the brain regions comprising different modules. Using an approach drawn from analysis of the (modular) global air transportation network (Guimerà et al., 2005), we classified every region in the brain networks as a connector node (having one or more inter-modular connections to nodes in other modules) or a provincial node (having only intra-modular connections to other nodes in the same module). We could then define a topological role for each module based on the proportion of connector nodes it contained. This showed that the three largest modules of the young brain network had rather different connector coefficients: posterior and central modules had relatively low intermodular connectivity, and no direct connections between them; whereas almost half of the regions comprising a fronto-cingulo-parietal module had connector status. This suggests that, in the young brain at least, the dorsal fronto-cingulo-parietal module, which also included striatal and thalamic regions, plays a critical role in coordinating activity across the brain network as a whole, and in mediating interactions between posterior (putatively visual) and central (putatively motor and auditory/verbal) modules. Thus the connector status of the fronto-cingulo-parietal module could be related to executive or attentional functions that are already known to depend on many of its component regions, such as dorsolateral prefrontal and medial posterior parietal cortex. It is also notable that regional components of the young fronto-cingulo-parietal module include medial frontal and posterior regions that have been identified as part of the “default mode” functional network (Greicius et al., 2003, Buckner et al. 2008) and that are known to be anatomically connected (Hagmann et al. 2008).

Second, we have directly compared the community structure of the large-scale functional networks of young adults to that of older healthy adults in an initial effort to characterise age-related changes in brain modularity. We found no significant difference between the two groups in terms of maximal modularity of the global network, implying that modular organization is conserved over the adult age range considered; but there were marked differences in the composition and topological roles of modules. Although some modules were almost identically composed in both age groups, notably the posterior and ventral frontal modules, the two largest modules in the young brain network were each represented by two smaller and more local modules in the older group's mean brain network. For example, the regions comprising the extensive fronto-cingulo-parietal network in the young brain network were segregated between a fronto-striato-thalamic and a medial posterior module in the older group's mean brain network. This more localized community structure was associated with significant changes in the distribution of intra- and inter-modular links in the older group's mean brain network. In particular, there were fewer intermodular connections to the fronto-striato-thalamic module from any posterior module, and there were more direct intermodular connections between posterior modules. The reduced connector status of the dorsal fronto-striatal module suggests that this system will not play a critical role in whole brain coordination, which is more likely to depend on the enhanced connector status of posterior modules, in the older group's mean brain network. This may have a bearing on cognitive changes linked to prefrontal dysfunction (West, 1996). There has been variable support for this hypothesis from functional neuroimaging studies, and mean activity in frontal regions can be increased or decreased in older adults (Grady et al., 1994, 1995). An intriguing and testable possibility attributes impairments in cognitive control not to changes in overall activity in frontostriatal regions but to qualitatively altered patterns of connectivity to other regions, as seen here.

The general notion that modularity of brain organization might change as a function of aging or maturation – a process sometimes described as modularization – has previously been proposed in the context of early (post-natal or childhood) brain development (Paterson et al., 1999). There have also been some interesting recent reports to suggest that topological reorganization of resting-state networks, specifically default mode components, may be ongoing and functionally important during the course of normal development from childhood to adulthood (Fair et al. 2007, 2008). However, to the best of our knowledge, these data provide the first empirical support for the hypothesis that maturational processes of brain modularization need

not be restricted to pre-adult life but might be ongoing as part of normal senescence. It is notable that some aspects of our results have been anticipated by prior imaging studies of aging. For example, the segregation of medial posterior and dorsal fronto-striatal modules in the older group's mean brain network is entirely in keeping with previous observations that functional connectivity between posterior cingulate and medial frontal cortical components of the "default mode" network is impaired in older subjects (Andrews-Hanna et al., 2007). There is also considerable, albeit less directly supportive, evidence from structural neuroimaging studies for attenuated white matter density or integrity in major axonal tracts subserving some of the long distance connections, e.g., between frontal and parietal cortex, included in the extensive fronto-cingulo-parietal module of the young brain network (O' Sullivan et al., 2001). However, there are also some limitations of the study which should inform interpretations of the observed differences. In general, the sample size is small thereby limiting power to detect group mean differences as well as possible group differences in variability (which would be expected theoretically to be greater in the older group). A more specific limitation is that we did not simultaneously monitor cardiac and respiratory cycles during fMRI data acquisition in these subjects. The use of wavelet filtering to restrict analysis of functional connectivity to a frequency interval of 0.06–0.11 Hz will have excluded very slow trends and higher frequencies directly corresponding to average cardiorespiratory cycles but we are limited in our capacity to exclude the possibility that observed differences in correlation between fMRI time series might reflect age-related differences in systemic blood flow, oxygenation or carbon dioxide levels. Likewise, there is some prior evidence for age-related differences in the form of the hemodynamic response function mediating the BOLD response in fMRI (D'Esposito et al. 2003) and this could conceivably have affected our results.

In conclusion, we have shown that human brain functional networks, derived from a connectivity analysis of fMRI data acquired in a no-task state, have a non-random modular organization or community structure. The topological roles of specific regions, defined in terms of the proportion of inter-modular connections each region makes with other regions outside its own module, were shown to vary between modules and in relation to normal aging. In young brain networks, most inter-modular connections involved regions of a fronto-cingulo-parieral module; whereas, in older adults, there were more numerous inter-modular connections to central and posterior modules. These observations are considered to be compatible with the hypothesis that developmental modularization – or maturational change in community structure of functional networks – may be an aspect of normal human adult brain aging.

Acknowledgments

This research was supported by a Human Brain Project grant from the National Institute of Mental Health and the National Institute of Biomedical Imaging & Bioengineering, National Institutes of Health, Bethesda, MD, USA. AM was supported by a Fellowship from Research into Aging, UK.

Appendix A. Supplementary data

Supplementary data associated with this article can be found, in the online version, at doi:10.1016/j.neuroimage.2008.09.062.

References

Achard, S., Bullmore, E., 2007. Efficiency and cost of economical brain functional networks. PLoS Comp. Biology 3, e17.
Achard, S., Salvador, R., Witcher, B., Suckling, J., Bullmore, E., 2006. A resilient, small-world human brain functional network with highly connected association cortical hubs. J. Neurosci. 26, 63–72.
Achard, S., Bassett, D.S., Meyer-Lindenberg, A., Bullmore, E., 2008. Fractal connectivity of long memory networks. Phys. Rev. E 77, 036104.
Andrews-Hanna, J., Snyder, A., Vincent, J., Lustig, C., Head, D., Raichle, M., Buckner, R., 2007. Disruption of large-scale brain systems in advanced aging. Neuron 56, 924–935.
Bassett, D.S., Bullmore, E.T., 2006. Small-world brain networks. Neuroscientist 12, 512–523.
Bassett, D.S., Meyer-Lindenberg, A., Achard, S., Duke, T., Bullmore, E., 2006. Adaptive reconfiguration of fractal small-world human brain functional networks. Proc. Natl. Acad. Sci. U. S. A. 103, 19518–19523.
Brandes, U., Delling, D., Gaertler, M., Goerke, R., Hoefer, M., Nikoloski, Z., Wagner, D., 2006. Maximizing modularity is hard. arXiv, physics 0608255.
Boccaletti, S., Ivanchenko, M., Latora, V., Pluchino, A., Rapisarda, A., 2007. Detecting complex network modularity by dynamical clustering. Phys. Rev. E 75, 045102.
Bollobas, B., 1985. Random Graphs. Academic Press, New York.
Buckner, R.L., Andrews-Hanna, J.R., Schacter, D.L., 2008. The brain's default network: anatomy, function and relevance to disease. Ann. NY Acad. Sci. 1124, 1–38.
Callebaut, W., Rasskin-Gutman, D., 2005. Modularity: Understanding the Development and Evolution of Natural Complex Systems. MIT Press, Cambridge USA.
Chen, Z.J., He, Y., Rosa-Neto, P., Germann, J., Evans, A.C., 2008. Revealing modular architecture of human brain structural networks by using cortical thickness from MRI. Cereb. Cortex 18, 2374–2381.
Clauset, A., Newman, M.E.J., Moore, C., 2004. Finding community structure in very large networks. Phys. Rev. E 70, 066111.
Cordes, D., Haughton, V.M., Arfanakis, K., Wendt, G.J., Turski, P.A., Moritz, C.H., Qugley, M.A., Meyerand, M.E., 2000. Mapping functionally related regions of brain with functional connectivity MR imaging. Am. J. Neuroradiol. 21, 1636–1644.
Cordes, D., Haughton, V., Carew, J.D., Arfanakis, K., Maravilla, K., 2002. Hierarchical clustering to measure connectivity in fMRI resting-state data. Magn. Reson. Imaging 20, 305–317.
Danon, L., Duch, J., Diaz-Guilera, A., Arenas, A., 2005. Comparing community structure identification. J. Stat. Mech. P09008.
D'Esposito, M., Deouell, L.Y., Gazzaley, A., 2003. Alterations in the BOLD fMRI signal with ageing and disease: a challenge for neuroimaging. Nat. Rev. Neurosci. 4, 863–872.
Fair, D.A., Dosenbach, N.U., Church, J.A., Cohen, A.L., Brahmbhatt, S., Miezin, F.M., Barch, D.M., Raichle, M.E., Petersen, S.E., Schlaggar, B.L., 2007. Development of distinct control networks through segregation and integration. Proc. Natl. Acad. Sci. U. S. A. 104, 13507–13512.
Fair, D.A., Cohen, A.L., Dosenbach, N.U., Church, J.A., Miezin, F.M., Barch, D.M., Raichle, M.E., Petersen, S.E., Schlaggar, B.L., 2008. The maturing architecture of the brain's default network. Proc. Natl. Acad. Sci. U. S. A. 105, 4028–4032.
Ferrarini, L., Veer, I.M., Baerends, E., van Tol, M.J., Renken, R.J., van der Wee, N.J.A., Veltman, D.J., Aleman, A., Zitman, F.G., Penninkx, B.W.J.H., van Buchem, M.A., Reiber, J.H.C., Rombouts, S.A.R.B., Milles, J., in press. Hierarchical functional modularity in the resting state human brain. Hum. Brain Mapp. (1 Oct 2008, Electronic publication ahead of print).
Fodor, J.A., 1983. The Modularity of Mind: An Essay on Faculty Psychology. MIT Press, Cambridge USA.
Folstein, M.F., Folstein, S.E., McHugh, P.R., 1975. Mini mental state. J. Psychiatry Res. 12, 189–198.
Grady, C., Maisog, J.M., Horwitz, B., Ungerleider, L., Mentis, M.J., Salerno, J.A., Pietrini, P., Wagner, E., Haxby, J.V., 1994. Age-related changes in cortical blood flow activation during visual processing of faces and locations. J. Neurosci. 14, 1450–1462.
Grady, C.L., McIntosh, A.R., Horwitz, B., Maisog, J.M., Ungerleider, L.G., Mentis, M.J., Pietrini, P., Schapiro, M.B., Haxby, J.V., 1995. Age-related reductions in human recognition memory due to impaired encoding. Science 269, 218–221.
Greicius, M.D., Krasnow, B., Reiss, A.L., Menon, V., 2003. Functional connectivity in the resting brain: a network analysis of the default mode hypothesis. Proc. Natl. Acad. Sci. USA 100, 253–258.
Guimerà, R., Amaral, L.A.N., 2005a. Cartography of complex networks: modules and universal roles. J. Stat. Mech. P02001.
Guimerà, R., Amaral, L.A.N., 2005b. Functional cartography of complex metabolic networks. Nature 433, 895–900.
Guimerá, R., Sales-Pardo, M., Amaral, L.A.N., 2004. Modularity from fluctuations in random graphs and complex networks. Phys. Rev. E 70, 025101.
Guimerà, R., Mossa, S., Turtschi, A., Amaral, L.A.N., 2005. The worldwide air transportation network: anomalous centrality, community structure, and cities' global roles. Proc. Natl. Acad. Sci. U. S. A. 102, 7794–7799.
Hagmann, P., Cammoun, L., Gigandet, X., Meuli, R., Honey, C.J., Wedeen, V.J., Sporns, O., 2008. Mapping the structural core of human cerebral cortex. PLoS Biol. 6, e159.
Hilgetag, C.C., Burns, G.A., O'Neill, M.A., Scannell, J.W., Young, M.P., 2000. Anatomical connectivity defines the organization of clusters of cortical areas in the macaque monkey and the cat. Philos. Trans. R. Soc. Lond. B Biol. Sci. 355, 91–110.
Kamada, T., Kawai, S., 1989. An algorithm for drawing general undirected graphs. Inform. Process. Lett. 31, 7–15.
Kashtan, N., Alon, U., 2005. Spontaneous evolution of modularity and network motifs. Proc. Natl. Acad. Sci. U. S. A. 102, 13773–13778.
Lowe, M.J., Mock, B.J., Sorenson, J.A., 1998. Functional connectivity in single and multislice echoplanar imaging using resting state fluctuations. NeuroImage 7, 119–132.
Massen, C.P., Doye, J.P.K., 2005. Identifying communities within energy landscapes. Phys. Rev. E 71, 046101.
Nelson, H.E., 1982. The National Adult Reading Test. NFER-Nelson, Windsor, UK.
Newman, M.E.J., 2004a. Detecting community structure in networks. Eur. Phys. J. B 38, 321–330.

Newman, M.E.J., 2004b. Fast algorithm for detecting community structure in networks. Phys. Rev. E 69, 066133.
Newman, M.E.J., 2006. Modularity and community structure in networks. Proc. Natl. Acad. Sci. U. S. A. 103, 8577–8582.
Newman, M.E.J., Girvan, M., 2004. Finding and evaluating community structure in networks. Phys. Rev. E 69, 026113.
O' Sullivan, M., Jones, D.K., Summers, P.E., Morris, R.G., Williams, S.C.R., Markus, H.S., 2001. Evidence for cortical "disconnection" as a mechanism of age-related cognitive decline. Neurology 57, 632–638.
Pan, R.K., Sinha, S., 2007. Modular networks emerge from multiconstraint optimization. arXiv, physics 0703033v2.
Paterson, S.J., Brown, J.H., Gsodl, M.K., Johnson, M.H., Karmiloff-Smith, A., 1999. Cognitive modularity and genetic disorders. Science 286, 2355–2358.
Radicchi, F., Castellano, C., Cecconi, F., Loreto, V., Parisi, D., 2004. Defining and identifying communities in networks. Proc. Natl. Acad. Sci. U. S. A. 101, 2658–2663.
Redies, C., Puelles, L., 2001. Modularity in vertebrate brain development and evolution. BioEssays 23, 1100–1111.
Reichardt, J., Bornholdt, S., 2006. When are networks truly modular? Physica D 224, 20–26.
Sales-Pardo, M., Guimerà, R., Moreira, A.A., Amaral, L.A.N., 2007. Extracting the hierarchical organization of complex systems. Proc. Natl. Acad. Sci. U. S. A. 104, 15224–15229.
Salvador, R., Suckling, J., Coleman, M., Pickard, J., Menon, D., Bullmore, E., 2005. Neurophysiological architecture of functional magnetic resonance images of human brain. Cereb. Cortex 15, 1332–1342.
Scannell, J.W., Blakemore, C., Young, M.P., 1995. Analysis of connectivity in the cat cerebral cortex. J. Neurosci. 15, 1463–1483.
Scannell, J.W., Burns, G.A.P.C., Hilgetag, C.C., O'Neill, M.A., Young, M.P., 1999. The connectional organization of the cortico-thalamic system of the cat. Cereb. Cortex 9, 277–299.
Schwarz, A.J., Gozzi, A., Bifone, A., 2008. Community structure and modularity in networks of correlated brain activity. Magn. Reson. Imaging 26, 914–920.
Stephan, K.E., Hilgetag, C.C., Burns, G.A.P.C., O'Neill, M.A., Young, M.P., Kötter, R., 2000. Computational analysis of functional connectivity between areas of primate cerebral cortex. Philos. Trans. R. Soc. Lond. B Biol. Sci. 355, 111–126.
Slotine, J.-J.E., Lohmiller, W., 2001. Modularity, evolution, and the binding problem: a view from stability theory. Neural Networks 14, 137–145.
Tzourio-Mazoyer, N., Landeau, N., Papathanassiou, B., Crivello, D., Etard, O., Delcroix, N., Mazoyer, B., Joliot, M., 2002. Automated anatomical labeling of activations in SPM using a macroscopic anatomical parcellation of the MNI MRI single-subject brain. NeuroImage 15, 273–289.
West, R.L., 1996. An application of prefrontal cortex function theory to cognitive aging. Psychol. Bull. 120, 272–292.
Whitcher, B., Guttorp, P., Percival, D.B., 2000. Wavelet analysis of covariance with application to atmospheric time series. J. Geophys. Res. 105, 941–962.
Young, M.P., 1992. Objective analysis of the topological organization of the primate visual cortical system. Nature 358, 152–155.
Zeki, S., Bartels, A., 1998. The autonomy of the visual systems and the modularity of conscious vision. Philos. Trans. Royal Soc. London B 353, 1911–1914.